Journal of Inflammation Research

Dovepress
Taylor & Francis Group

Open Access Full Text Article

ORIGINAL RESEARCH

PLK1 Mediates the Proliferation and Contraction of Airway Smooth Muscle Cells and Has a Role in T2-High Asthma with Neutrophilic Inflammation Model

Yilin Pan[1,*], Yishu Xue[1,*], Xia Fei[1,*], Lei Zhao[1,*], Lei Han[1], Hang Su[1], Yanmei Lin[1], Yan Zhou[1], Yingying Zhang[1], Guogang Xie[1], Deping Kong[2], Wuping Bao[1], Min Zhang[1]

[1]Department of Respiratory and Critical Care Medicine, Shanghai General Hospital, Shanghai Jiao Tong University School of Medicine, Shanghai, People's Republic of China; [2]Precision Research Center for Refractory Diseases, Institute for Clinical Research, Shanghai General Hospital, Shanghai Jiao Tong University School of Medicine, Shanghai, People's Republic of China

*These authors contributed equally to this work

Correspondence: Min Zhang; Wuping Bao, Department of Respiratory and Critical Care Medicine, Shanghai General Hospital, Shanghai Jiao Tong University School of Medicine, No. 100, Haining Road, Shanghai, 200080, People's Republic of China, Email zhangmin@sjtu.edu.cn; wupingbao1982@163.com

Background: Type 2 (T2)-high asthma with neutrophilic inflammation is characterized by airway eosinophilic and neutrophilic infiltration, hyperresponsiveness, remodeling, and insensitivity to steroid treatment. Sphingosine-1-phosphate (S1P), which has a crucial role in the development of asthma, promotes the proliferation and contraction of airway smooth muscle cells (ASMCs), contributing to the pathophysiological processes of asthma. However, the downstream mediator of S1P remains unclear, as does its role in T2-high asthma with neutrophilic inflammation.

Methods: Ovalbumin- and ozone-induced murine models were used to replicate T2-high asthma with neutrophilic inflammation and primary ASMCs were applied to explore the underlying effects. Through transcriptomic analysis, PLK1 was identified as a potential key molecule associated with S1P-induced proliferation and contraction. Functional studies were performed both in vitro and in vivo by pharmacological inhibition to validate the role of PLK1 and to evaluate the therapeutic effects of PLK1 inhibition.

Results: S1P level was elevated in the bronchoalveolar lavage fluid (BALF) of T2-high asthma with neutrophilic inflammation model, and promoted ASMCs proliferation and contraction. PLK1 expression increased in S1P-stimulated ASMCs and asthmatic lung tissues. Inhibition of PLK1 blocked S1P-induced ASMCs proliferation and contraction. In vivo, PLK1 inhibition reduced airway inflammation (particularly neutrophilic infiltration), airway remodeling (airway smooth muscle proliferation and collagen deposition), and airway hyperresponsiveness and resistance, improving lung function (of both large and small airways), with superior therapeutic effects to those of dexamethasone. In addition, PLK1 inhibition markedly reduced the BALF levels of IL-17A, IL-21 and IL-6, suggesting that PLK1 might exert its effects mainly through the regulation of Th17 pathway.

Conclusion: PLK1 mediates S1P-induced ASMC proliferation and contraction, and plays an important part in T2-high asthma with neutrophilic inflammation model, making it a potential therapeutic target for treating T2-high asthma with neutrophilic inflammation.

Keywords: T2-high asthma with neutrophilic inflammation, PLK1, airway smooth muscle cells, S1P, volasertib

Introduction

Asthma is a chronic airway disease characterized by airway inflammation, hyperresponsiveness, and remodeling that affects >300 million patients worldwide.[1] Based on different pathophysiological mechanisms, asthma is currently classified into type-2 (T2)-high asthma and T2-low (non-T2) asthma. T2-high asthma accounts for a large proportion of asthma cases, and the endotype with concurrent airway neutrophilic inflammation is gaining increasing attention due to its severe airway remodeling, airway responsiveness and poor respond to steroid treatment.[2,3] Airway smooth muscle

Received: 17 December 2024
Accepted: 14 March 2025
Published: 25 March 2025

cells (ASMCs) are key cells in the asthma process. During the course of asthma, ASMCs exhibit enhanced proliferation and contraction, leading to airway remodeling and increased airway hyperresponsiveness.

Sphingosine-1-phosphate (S1P) is a membrane sphingolipid that activates various signaling pathways through S1P receptors (S1PRs) to promote cell survival, proliferation, migration, etc.[4] The S1P signaling pathway participates in the pathogenesis of asthma, and elevated levels of S1P have been detected in the bronchoalveolar lavage fluid (BALF) and serum of asthma patients.[5,6] Reinke et al found that S1P metabolism levels were closely related to severity of asthma,[7] and S1P has been reported to induce secretion of IL-8, enhancing neutrophil chemotaxis and driving neutrophilic inflammation in the airways.[8] Direct injection of S1P causes asthma-like features,[9] whereas pharmacological inhibition of sphingosine kinase 1 (an enzyme that catalyzes S1P) or $S1PR_2$ inhibits airway inflammation, hyperresponsiveness, and remodeling in asthma models.[10,11] Further research has shown that S1P promotes proliferation and contraction of ASMCs in vitro;[12,13] however, the mechanism underlying the effects of S1P on ASMC remains unclear.

Our previous research found that ozone exposure enhances airway neutrophil infiltration in ovalbumin (OVA)-sensitized and challenged asthmatic mice.[14] Furthermore, we confirmed that this model exhibited increased airway hyperresponsiveness, airway inflammation (particularly neutrophilic inflammation), and airway remodeling, with reduced responsiveness to steroid treatment, simulating T2-high asthma with neutrophilic inflammation to some extent.[15] In addition, we demonstrated that S1P promoted ASMC proliferation through $S1PR_{2/3}$, but the downstream molecule mediating this effect remained unclear.[16] In the present study, we aimed to determine: (1) which molecule mediates the effects of S1P on ASMCs; (2) the impact on ASMCs of targeting this molecule; and (3) whether targeting this molecule could treat our previously established the OVA + ozone-induced T2-high asthma with neutrophilic inflammation model.

Materials and Methods

Animals, Grouping, and OVA Sensitization/Challenge and Ozone Exposure Protocols

This study was approved by the Ethics Committee at Shanghai General Hospital, China (IACUC: 2023AW334). C57BL/6 mice (specific pathogen free; aged 6–8 weeks; male) were purchased from SLRC Laboratory (Shanghai, China) and housed under controlled conditions, with temperature maintained at 21–25 °C and humidity at 40–60%. They had ad libitum access to water and food free from OVA. The mice underwent a 7-day acclimatization period before experimentation and were maintained on a 12-h light/dark cycle.

Mice were randomly divided into five groups (control, volasertib, OVA + ozone, OVA + ozone + dexamethasone (Dex), and OVA + ozone + volasertib). On days 0 and 7, OVA sensitization was initiated by intraperitoneal injection of OVA (5 mg/kg; grade V; Sigma-Aldrich, USA) dissolved in 0.2 mL of phosphate-buffered saline (PBS) and emulsified with aluminum hydroxide (2%) as an adjuvant. On days 14, 16, 18, 20, and 22, OVA challenge was undertaken by exposure to 1.5% aerosolized OVA (10 mL) in a plastic box linked to an ultrasonic nebulizer (Clenny 2 Aerosol; Medel, Italy) for 30 min. Mice in the control group were sensitized and challenged with an identical volume (0.2 mL for sensitization and 10 mL for challenge) of PBS as vehicle. Mice were exposed to ozone (2.5 ppm) or air for 2 h in a Perspex™ container 30 min after each OVA/PBS challenge on days 14, 16, 18, 20, and 22. Ozone was produced by an ozonizer (300 series; Aqua Medic, Germany). The ozone concentration was continuously controlled and adjusted with an OS-4 ozone switch (Ecosensor; KWJ Engineering, USA). Mice in the control group were exposed to air during this time. Mice were intraperitoneally injected with volasertib (5 mg/kg), or Dex (5 mg/kg), or vehicle (10% dimethyl sulfoxide and 20% SBE-β-CD in saline) 30 min before the OVA challenge on days 14, 16, 18, 20 and 22.

Cell Preparation and Culture

Primary ASMCs from tracheas and main bronchi of C57BL/6 (15–20 g) were isolated as previously described.[17] All animal procedures were performed in accordance with the Guide for the Care and Use of SLRC Laboratory (Shanghai, China). Briefly, the tracheas and main bronchi were rapidly removed from mice, washed in PBS (4 °C) and then dipped into Dulbecco's modified Eagle medium (DMEM; Gibco, USA) with 10% fetal bovine serum (FBS; Sijiqing, China), 100 U/mL penicillin, and 100 μg/mL streptomycin. The serosa and epithelium were carefully stripped off using fine forceps and a surgical blade. Next, the remaining tissue was cut into 0.5-mm pieces, placed into a culture flask, and incubated at

37 °C in an atmosphere of 95% air and 5% CO_2. Cells were fed every 2–3 days and passaged by trypsinization using 0.25% trypsin (Invitrogen, USA) until they reached 70–80% confluence. Immunofluorescence staining with α-smooth muscle actin (α-SMA; Proteintech, China) confirmed that the cultured cells were more than 95% ASMCs. Before each experiment, cells were incubated with 1% FBS–DMEM overnight to minimize serum-induced effects. S1P (MedChemExpress, USA) was used to stimulate ASMCs, and volasertib (BI 6727) (100nM, MedChemExpress, USA) was used to inhibit PLK1.

Cell Proliferation Assay

Cell proliferation was determined using a BrdU ELISA Kit (Maibio, China) according to the manufacturer's instructions. Briefly, cells were seeded into 96-well plates at a density of 5×10^3 cells per well, allowed to adhere for at least 24 h, and serum starved overnight (1% FBS in DMEM) before the start of the experiments. BrdU labeling reagent was added to the wells, followed by incubation for 2 h at 37 °C. Next, cells were denatured with FixDenat solution for 30 min at room temperature, then incubated with anti-BrdU monoclonal antibodies conjugated to peroxidase for 90 min at room temperature. The antibody conjugate was removed, and substrate solution was added and allowed to react for 10 min. The absorbance at 370 nm was determined using a microplate reader (Bio-Rad, USA). The blank consisted of 100 μL culture medium with or without BrdU.

Collagen Gel Contraction Assay

ASMCs were resuspended in a collagen solution that was prepared using cold collagen type I (purity ≥90%, liquid in 0.02 N acetic acid; 1.5 mg/mL, CORNING, USA) containing cells (2.0×10^5 cells/well). The gels were added to 24-well plates (600 μL/well) and left to polymerize at 37 °C for 60 min. Then, 0.5 mL DMEM containing 10% FBS was added to each well of a 24-well plate, followed by incubation at 37 °C for 48 h to allow mechanical load to develop. S1P was added to appropriate wells to a final concentration of 1 μM with or without pretreatment with volasertib (100 nM) for 1 h. Collagen matrices were released from the edges of the wells, removing isometric load, to initiate contraction. Matrix contraction was allowed to proceed for 24 h at 37 °C in the presence of the indicated reagents. The surface area of each gel was measured using ImageJ.

RNA Sequencing Sample Preparation and Analysis

RNA was extracted using an RNeasy Mini Kit (QIAGEN, Germany), and libraries were constructed using a NEBNext® Ultra™ RNA Library Prep Kit for Illumina® (#E7530L, NEB, USA). The libraries were then combined and subjected to 150-bp paired-end sequencing on an Illumina NovaSeq 6000 system at Annoroad Gene Technology Company (Beijing, China). Data from samples acquired through Illumina high-throughput sequencing were stored as image files. Base calling was performed using CASAVA to convert the data into sequences of reads. The resulting high-quality reads were subsequently aligned to the reference genome with the aid of HISAT2.

Quantitative Real-time Polymerase Chain Reaction (qRT-PCR)

Total RNA was extracted from lung tissues using TRIzol™ reagent (Invitrogen, USA) and subsequently converted to complementary DNA with a cDNA Reverse Transcription Kit (Applied Biosystems, USA) in a PTC-200 Peltier Thermal Cycler (MJ Research, USA). A ViiA™ 7 Real-Time PCR System (Thermo Fisher, USA) was employed for RT-qPCR analysis. Fluorescence intensity was recorded for both the internal reference gene (β-actin) and the target gene (PLK1). Relative expression levels of target genes were determined using the $2^{-\Delta\Delta Ct}$ method. The primers used for PCR were 5′-GGCAACCAAAGTGGAATATG-3′ and 5′-CAGCACCTCAGGAGCTATGTA-3′ for PLK1, and 5′-CCTCTATGCC AACACAGT-3′ and 5′-AGCCACCAATCCACACAG-3′ for β-actin.

Immunoblotting

Total proteins were extracted with RIPA lysis buffer (Epizyme Biotech, China), and protein concentration was determined using a BCA protein assay kit (Epizyme Biotech). Proteins were separated by sodium dodecyl sulfate polyacrylamide gel electrophoresis and transferred to a Trans-Blot polyvinylidene difluoride membrane (MILLIPORE, USA),

and relative expression of proteins was determined using an ECL detection system. The primary antibodies were against PLK1 (ab17057; Abcam, USA) and β-actin (LF201; Epizyme Biotech, China).

Lung Histology and Immunohistochemical Analyses

After resection of mouse lungs, the left lungs were inflated by injection of 4% paraformaldehyde to provide 20 cm of water pressure. They were then immersed overnight in paraformaldehyde and embedded in paraffin before being sectioned. Lung sections were stained with hematoxylin/eosin for airway inflammation and with Masson trichrome for collagen deposition. The slides were incubated with antibodies against PLK1 (10305-1-AP; Proteintech, China) or α-SMA (GB111364-100; Servicebio, China). Sections were examined using a light microscope and quantified using ImageJ software (MD, USA). Inflammation scores and Masson-stained, PLK1-stained, or α-SMA-stained areas were evaluated using Image J in a double-blind manner by two investigators independently.

Spirometry in Mice Using a Forced Maneuvers System

Twenty-four hours after the last OVA challenge, mice were anesthetized, fitted with a tracheal cannula, and attached to a plethysmograph with a pneumotachograph using the eSpira Forced Manoeuvres System for mice (EMMS, Hants, UK) to mimic classical clinical spirometry as previously described.[15] Variables including forced vital capacity (FVC), volume expired in the first 25 ms of fast expiration (FEV_{25}), FEV50, FEV75, FEF25 (forced expiratory flow at 25% of FVC), FEF50, FEF75, and maximal mid-expiratory flow (MMEF) were calculated; of these variables, FEV25, FEV50, FEV75, and FEF25 represented large-airway function, whereas FEF50, FEF75, and MMEF represented small-airway function.[18]

Airway Responsiveness

The anesthetized mice were then ventilated (MiniVent, Hugo Sachs Electronik, Germany) in a whole-body plethysmograph with a pneumotachograph linked to a differential pressure transducer (EMMS, Hants, UK) as previously described.[15] Airway resistance (R_L) was recorded for 3 min at each concentration of inhaled acetylcholine chloride (ACh, Sigma-Aldrich, USA) (4–256 mg/mL, 10 μL each time). R_L was expressed as the percentage change from baseline R_L (measured following PBS nebulization). The ACh concentration required to increase R_L by 100% from baseline (PC_{100}) was calculated, and $-\log PC_{100}$ was used as an indicator of AHR.

BALF Measurements

The tracheas of the anesthetized mice were accessed to collect BALF via infusion of 0.6 mL PBS three times through a polyethylene (PE-60) tube. The BALF recovery rate was above 80%. The reclaimed BALF was centrifuged at 3000 rpm for 10 min at 4 °C. Total cell counts were calculated using a hemocytometer under an optical microscope. Supernatants were collected for measurement of levels of S1P, IL-4, IL-5, IL-6, IL-13, IL-17A, and IL-21 via ELISA using kits (for S1P: Echelon Biosciences, USA; for IL-4, IL-5, IL-6, IL-17A: ANOGEN, Canada; for IL-13, IL-21: Invitrogen, USA) following the manufacturers' protocols.

Statistical Analysis

All experiments were repeated at least three times. All data are presented as mean ± standard deviation. Data were analyzed using one-way analysis of variance with Tukey's post hoc test by SPSS 13.0 software (SPSS Inc., Chicago, IL, USA). $P < 0.05$ was considered to indicate statistical significance.

Results

S1P Increased in BALF of OVA + Ozone Group and Stimulated Proliferation and Contraction of ASMCs in vitro

We established a T2-high asthma with neutrophilic inflammation using OVA + ozone as previously described.[15] The OVA + ozone group exhibited more airway inflammation, subepithelial collagen fiber deposition, and bronchial muscularization than the control group (Figure 1A–D). S1P level in the BALF of the OVA + ozone-induced T2-high

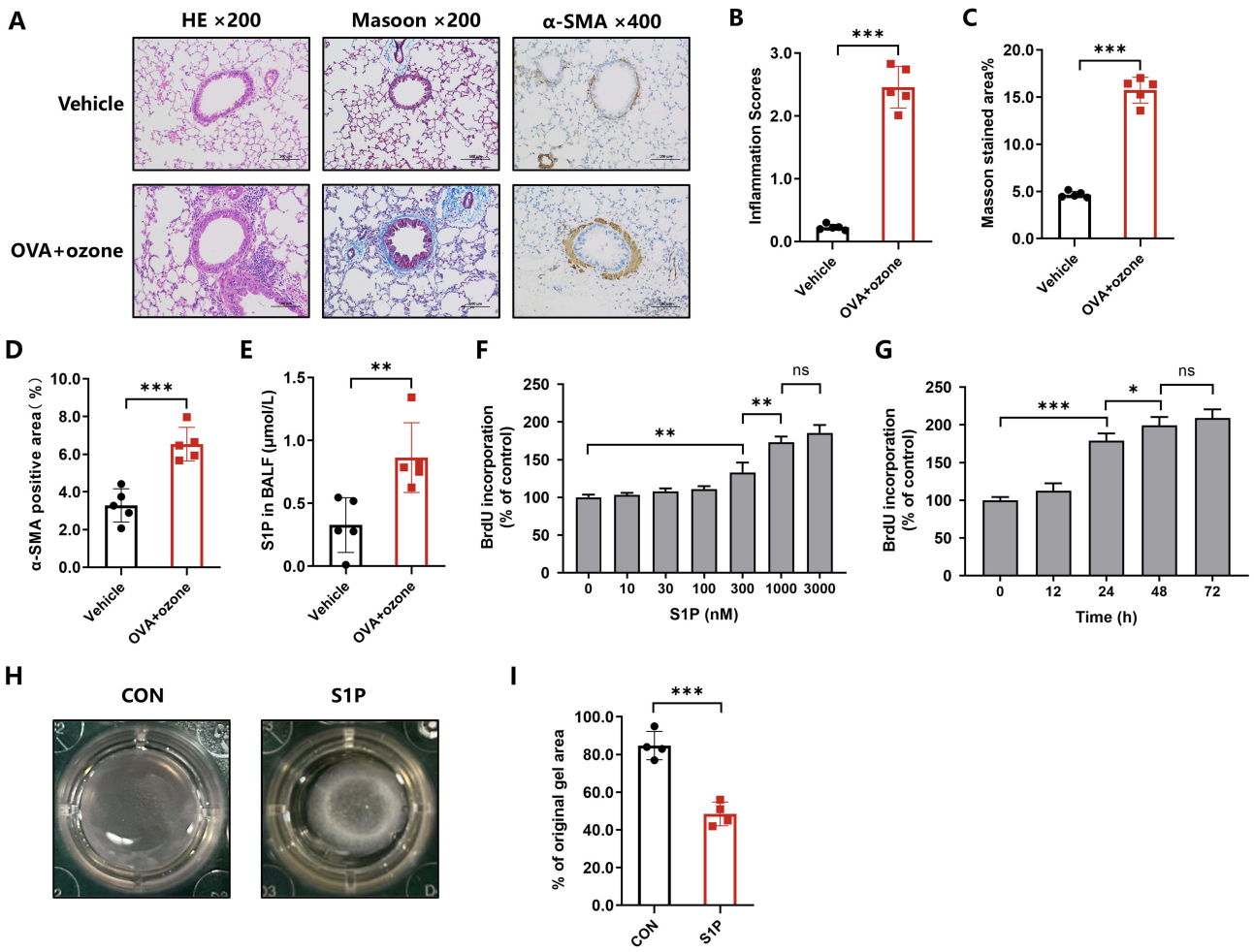

Figure 1 Increased S1P levels in BALF of T2-high asthma with neutrophilic inflammation model and stimulation of ASMC proliferation and contraction. (**A**) Representative photomicrographs of lung with inflammatory cell infiltration, airway collagen deposition, and α-SMA in lung-tissue slices. Scale bar, 100 μm. (**B**) Airway inflammation scores (n = 5 per group). (**C**) Percentage of subepithelial Masson stained area (n = 5 per group). (**D**) Percentage α-SMA-positive area around airways (n = 5 per group). (**E**) S1P levels in BALF from vehicle control mice and OVA + ozone mice (n = 5 per group). (**F**) Rate of BrdU incorporation in ASMCs stimulated with different concentrations of S1P for 24 h (n = 4 per group). (**G**) Rate of BrdU incorporation in ASMCs stimulated with 1 μM S1P for the indicated times (n = 4 per group). (**H** and **I**) Representative images of gel contraction. Collagen matrices containing ASMCs were incubated in the presence of S1P (1 μM); after 24 h of treatment, the contraction of the collagen gel was measured (n = 4 per group). The error bars represent the standard deviation. *P < 0.05, **P < 0.01, ***P < 0.001.
Abbreviation: ns, not significant.

asthma with neutrophilic inflammation model was significantly elevated (Figure 1E). To examine the effects of S1P on proliferation of ASMCs, cells were treated with S1P at different concentrations (0, 10, 30, 100, 300, 1000, 3000 nM) or for different times (0, 12, 24, 48, 72 h), and cell proliferation was measured using BrdU incorporation assay. As shown in Figure 1F, S1P stimulated proliferation of ASMCs in a dose-dependent manner, and 1 μM S1P triggered a 1.73-fold increase in BrdU incorporation in 24 h. Moreover, the results shown in Figure 1G indicated that S1P stimulated ASMC proliferation in a time-dependent manner, and 1 μM S1P caused a 2.09-fold increase in BrdU incorporation compared with controls at the time point of 72 h. As these findings suggested that S1P stimulates ASMCs proliferation in a concentration- and time-dependent manner, we chose 1 μM and 24 h as the S1P concentration and stimulation time for subsequent experiments. In addition, we examined the effects of S1P (1 μM, 24 h) on ASMC contraction using collagen gel contraction assays. As shown in Figure 1H and I, S1P caused a potent contraction of ASMC-embedded collagen gel, with the gel surface area reducing by 52%, compared with 15% in the control group (P < 0.001). Taken together, these data suggest that S1P increased in the T2-high asthma with neutrophilic inflammation model and effectively stimulated proliferation and contraction of ASMCs.

https://doi.org/10.2147/JIR.S501645

PLK1 Might Be an Important Downstream Molecule in the S1P Signaling Pathway

To further clarify which downstream molecule mediated the effects of S1P on ASMCs, we performed transcriptomic analyses using RNA sequencing to identify genes with significantly altered expression after stimulation with S1P (1 μM, 24 h). As shown in the heatmap, we observed that *Plk1* was highly upregulated among the transcripts, which encodes a kinase linked to hyperproliferation of highly invasive cancer cells,[19] as well as contraction of prostate smooth muscle[20] (Figure 2A). Moreover, PLK1 pathway was significantly upregulated in S1P-stimulated ASMCs compared with control ASMCs according to the Pathway Interaction Database (PID) enrichment analysis (Figure 2B).

PLK1 Mediated S1P-Induced Proliferation and Contraction of ASMCs

We next examined whether levels of PLK1 changed as indicated by the sequencing results. As shown in Figure 3A and B, PLK1 mRNA and protein levels significantly increased in ASMCs after S1P stimulation. Then, to determine whether PLK1 mediated S1P-induced proliferation and contraction of ASMCs, we applied selective PLK1 antagonist volasertib (100 nM) for 1 h before stimulation of cells with S1P. As shown in Figure 3C, volasertib did not affect the normal proliferation of ASMCs, consistent with previous research.[19] However, the presence of volasertib suppressed the ability of S1P (1 μM, 24 h) to trigger ASMCs proliferation; the rate of BrdU incorporation declined from 1.78-fold to 1.09-fold compared with controls ($P < 0.001$ versus S1P-treated cells). The contraction of ASMCs was also inhibited by volasertib (Figure 3D and E). Taken together, these results reveal that PLK1 plays a key role in inducing the proliferation and contraction of ASMCs.

PLK1 Was Overexpressed in T2-High Asthma with Neutrophilic Inflammation Model

To clarify the changes of PLK1 in the T2-high asthma with neutrophilic inflammation model, we measured PLK1 mRNA and protein levels in lung tissues. As expected, there were marked increases in levels of PLK1 mRNA and protein in the lung tissues of the OVA + ozone-induced T2-high asthma with neutrophilic inflammation model compared with those of the control group (Figure 4A and B). The PLK1-positive area in the lung tissues was also increased in the OVA + ozone group compared with the control group (Figure 4C and D).

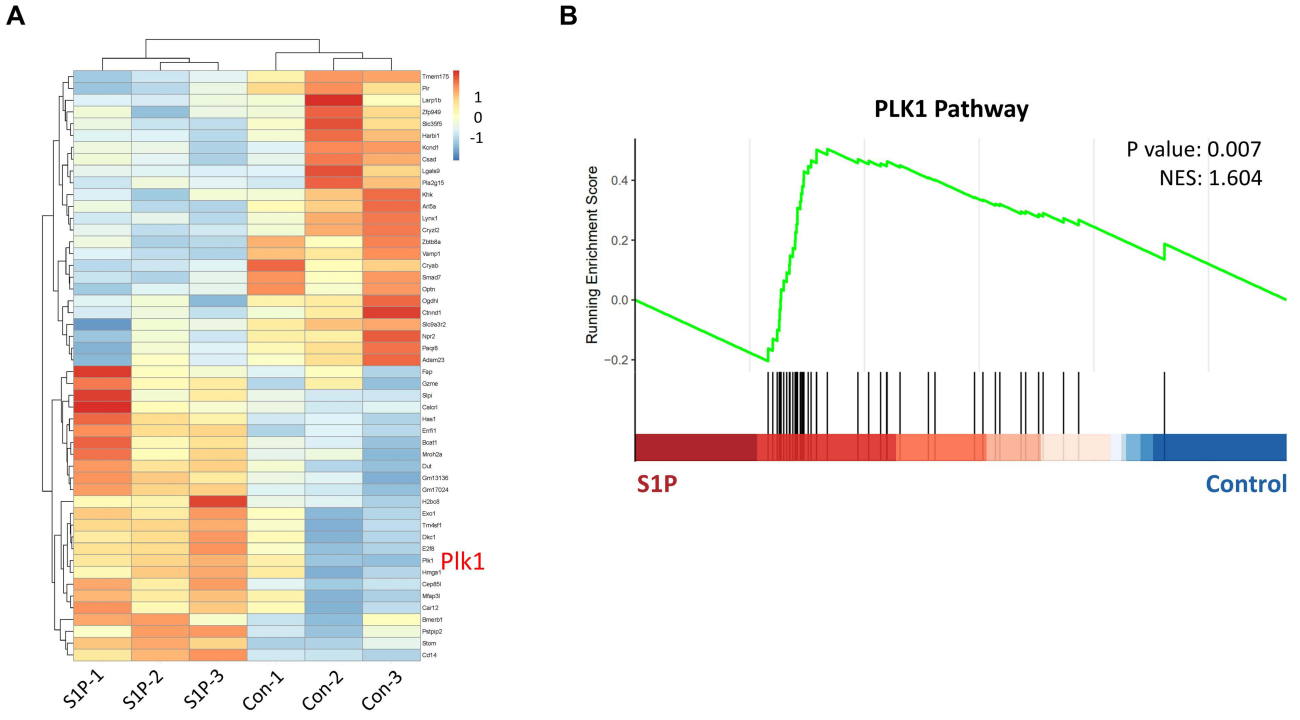

Figure 2 Transcriptomic sequencing analysis. (**A**) Heatmap of gene expression in ASMCs with or without S1P-treatment. (**B**) Pathway Interaction Database enrichment analysis of gene expressions in ASMCs with or without S1P-treatment.

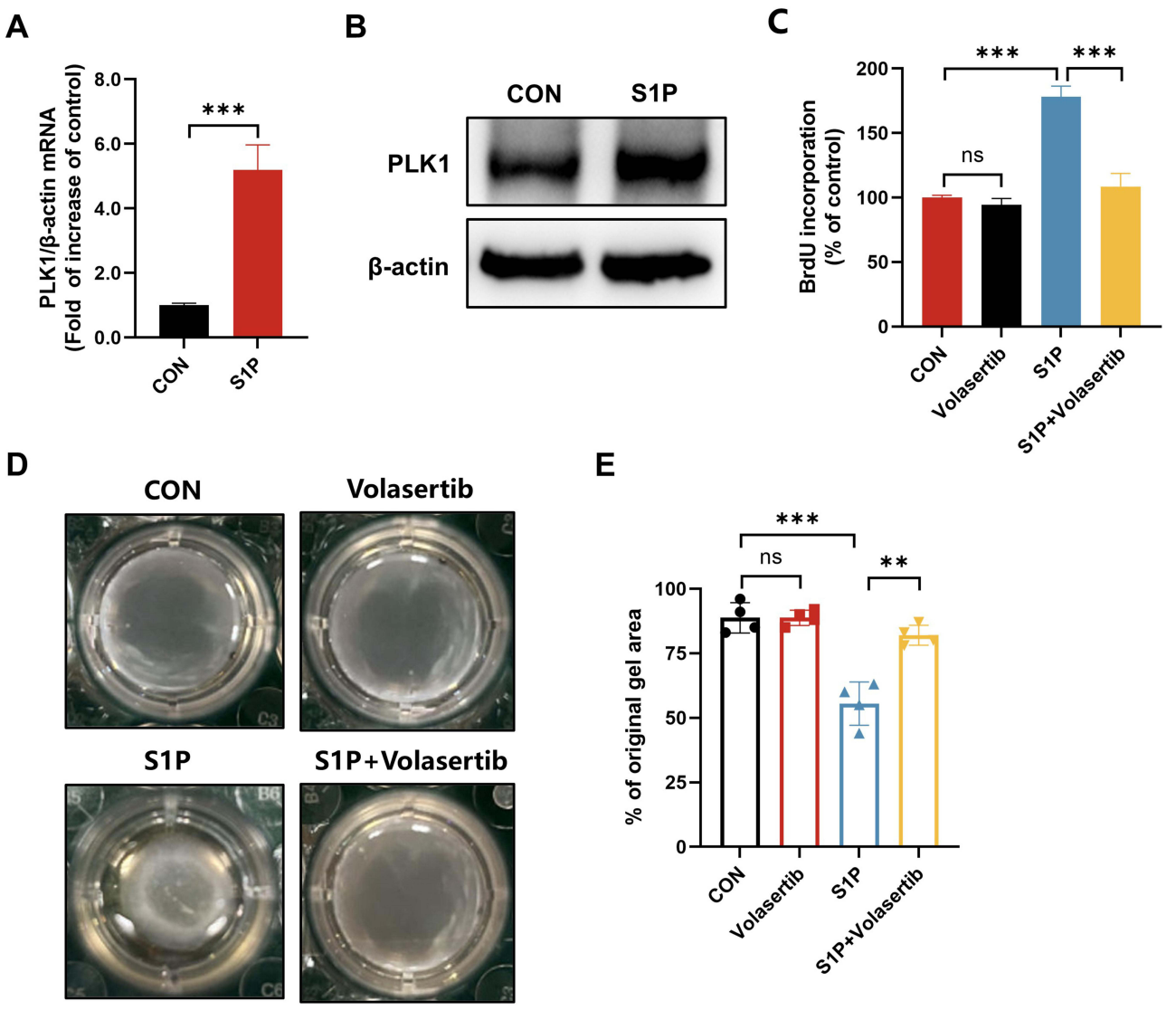

Figure 3 PLK1 mediation of S1P-induced proliferation and contraction of ASMCs. (**A**) PLK1 mRNA levels in ASMCs with or without S1P stimulation (n = 4 per group). (**B**) PLK1 protein levels in ASMCs with or without S1P stimulation (n = 4 per group). (**C**) Rate of BrdU incorporation in ASMCs with or without S1P stimulation and with or without volasertib treatment (n = 4 per group). (**D** and **E**) Representative images of gel contraction. Collagen matrices containing ASMCs were pretreated with volasertib for 1 h before S1P stimulation for 24 h, and the collagen gel contraction was measured (n = 4 per group). The error bars represent the standard deviation. **P < 0.01, ***P < 0.001.
Abbreviation: ns, not significant.

PLK1 Inhibition Improved Lung Function and Attenuated Airway Hyperresponsiveness, Inflammation, and Remodeling in T2-High Asthma with Neutrophilic Inflammation Model

To further investigate the roles of PLK1 in the T2-high asthma with neutrophilic inflammation model, we treated the OVA + ozone model with PLK1 inhibitor volasertib and compared its therapeutic effects with those of Dex. Large-airway function was assessed based on FEV25/FVC and FEV50/FVC values, whereas small-airway function was assessed by MMEF, FEF50, and FEF75. The T2-high asthma with neutrophilic inflammation models showed both large- and small-airway dysfunction, as described previously.[21] There were no obvious effects of Dex treatment in these models; however, PLK1 inhibition significantly improved both large and small-airway function (Figure 5A–E). The T2-high asthma with neutrophilic inflammation models also exhibited a leftward shift in the concentration responsiveness curve for R_L (Figure 5F), as well as reduced $-\log PC_{100}$ values compared with control (Figure 5G), suggesting increased airway resistance and airway hyperresponsiveness. Compared with

https://doi.org/10.2147/JIR.S501645

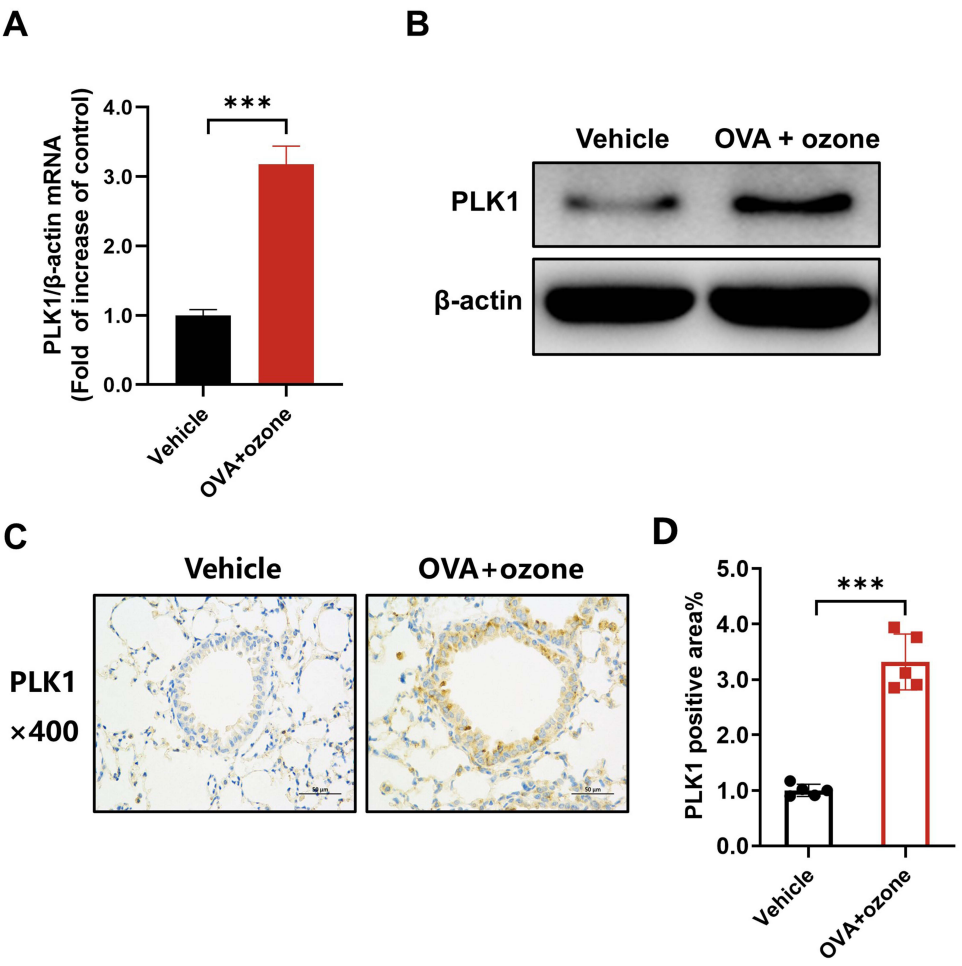

Figure 4 Overexpression of PLK1 in T2-high asthma with neutrophilic inflammation model. (**A**) PLK1 mRNA levels in lung tissue from vehicle control mice and OVA + ozone mice (n = 5 per group). (**B**) PLK1 protein levels in lung tissue from vehicle control mice and OVA + ozone mice (n = 5 per group). (**C**) Representative photomicrographs of immunohistochemistry of PLK1 in lung-tissue slices from vehicle control mice and OVA + ozone mice. Scale bar, 50 μm. (**D**) Percentage PLK1-positive area around airways (n = 5 per group). The error bars represent the standard deviation. ***P < 0.001.

Dex treatment, inhibition of PLK1 markedly alleviated airway hyperresponsiveness and airway resistance in T2-high asthma with neutrophilic inflammation models (Figure 5F and G).

The OVA + ozone group exhibited more airway inflammation, subepithelial collagen fiber deposition, and bronchial muscularization, as well as higher numbers of total cells, neutrophils, and eosinophils compared with the control group (Figure 5H–P). Following inhibition of PLK1, airway inflammation, subepithelial collagen fiber deposition, bronchial muscularization, and numbers of neutrophils and eosinophils in T2-high asthma with neutrophilic inflammation model were all reduced. Compared to Dex, the anti-inflammatory effect of volasertib was comparable (Figure 5H and K), and it showed more pronounced effects against collagen deposition (Figure 5I and L), airway muscularization (Figure 5J and M), and airway neutrophil infiltration (Figure 5O).

Effects of PLK1 Inhibition on Inflammatory Cytokines Levels in BALF of T2-High Asthma with Neutrophilic Inflammation Model

BALF levels of Th2-related cytokines IL-4, IL-5, and IL-13; Th17-related cytokines IL-17A, and IL-21; and inflammation-related cytokine IL-6 were elevated in T2-high asthma with neutrophilic inflammation models compared with the control group (Figure 6A–F). Dex could reduce the levels of IL-4 and IL-13, but has little effect on IL-5, IL-17A, IL-21, or IL-6. However, inhibition of PLK1 reduced BALF IL-5 and IL-6 levels of T2-high asthma with neutrophilic inflammation models

but had little effect on IL-4 or IL-13. There were significant decreases in levels of IL-17A and IL-21 in T2-high asthma with neutrophilic inflammation models treated with volasertib.

Discussion

This study identified PLK1 as a key downstream molecule of S1P signaling, with a role in inducing ASMC proliferation and contraction, and showed that it is critically involved in T2-high asthma with neutrophilic inflammation. PLK1 mediates S1P-induced ASMC proliferation and contraction. Inhibition of PLK1 significantly reduced airway inflammation in the T2-high asthma with neutrophilic inflammation model, particularly neutrophil infiltration, while also

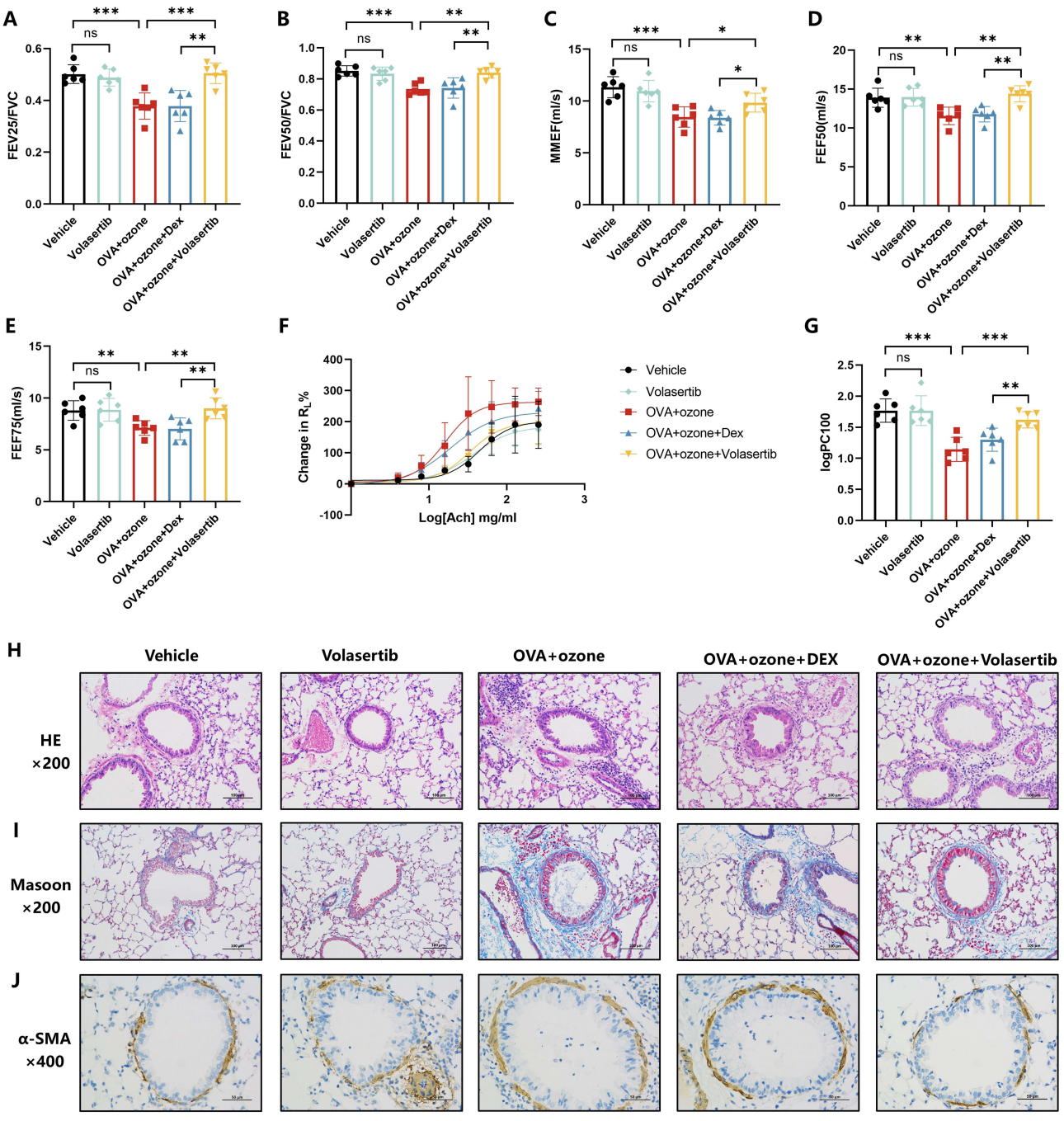

Figure 5 Continued.

https://doi.org/10.2147/JIR.S501645

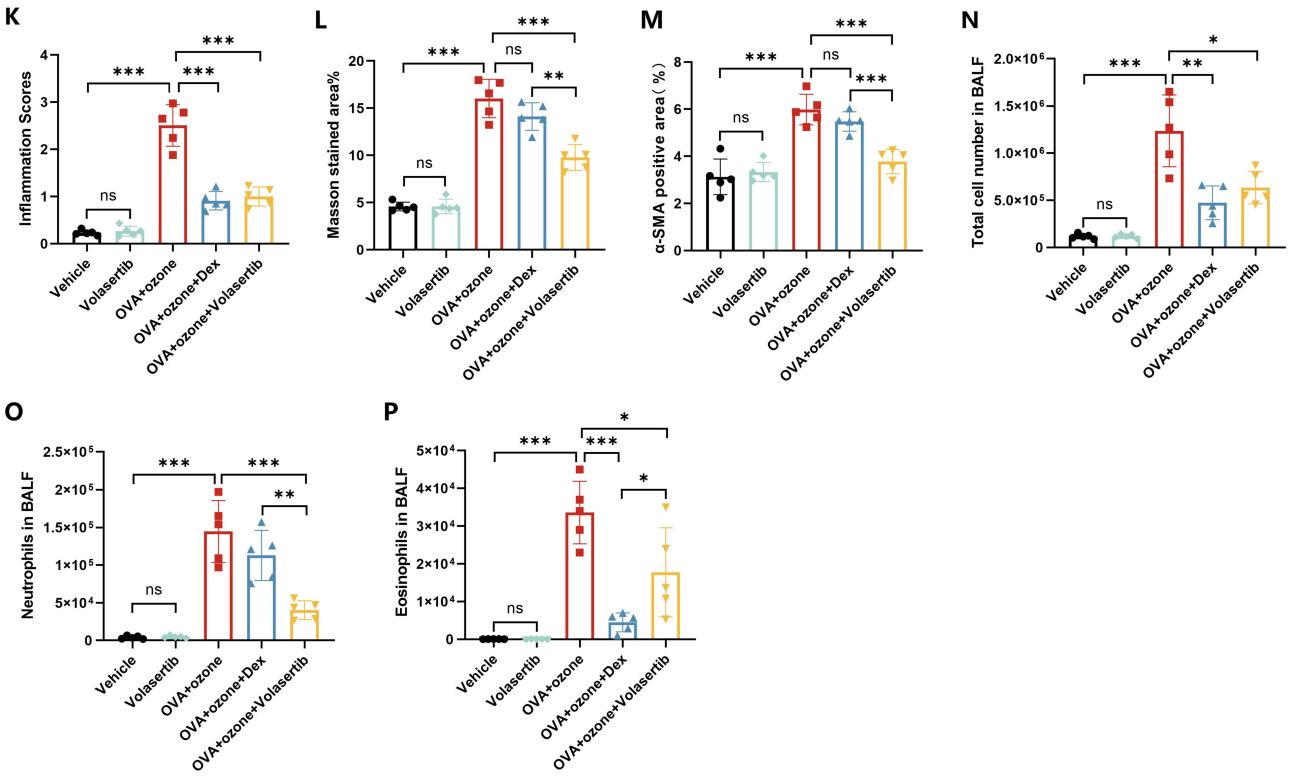

Figure 5 Effects of PLK1 inhibition on lung function, airway hyperresponsiveness, inflammation, and remodeling in T2-high asthma with neutrophilic inflammation model. (**A** and **B**) Large-airway function indicators (FEV_{25}/FVC, FEV_{50}/FVC) (n = 6 per group). (**C–E**) Small-airway function indicators (MMEF, FEF_{50}, FEF_{75}) (n = 6 per group). (**F**) Mean percentage increase in R_L in response to increasing concentrations of Ach (n = 6 per group). (**G**) $-logPC_{100}$ (ACh concentration required to increase R_L by 100% from baseline) (n = 6 per group). (**H**) Representative photomicrographs of lung with inflammatory cell infiltration. Scale bar, 100 μm. (**I**) Representative photomicrographs of lung with airway collagen deposition. Scale bar, 100 μm. (**J**) Representative photomicrographs of immunohistochemistry of α-SMA in lung-tissue slices. Scale bar, 50 μm. (**K**) Airway inflammation scores (n = 5 per group). (**L**) Percentage of subepithelial Masson stained area (n = 5 per group). (**M**) Percentage α-SMA-positive area around airways (n = 5 per group). (**N**) Total cell numbers in BALF (n = 5 per group). (**O**) Numbers of neutrophils in BALF (n = 5 per group). (**P**) Numbers of eosinophils in BALF (n = 5 per group). The error bars represent the standard deviation. *P < 0.05, **P < 0.01, ***P < 0.001.

Abbreviations: ACh, acetylcholine chloride; R_L, lung resistance; BALF, bronchoalveolar lavage fluid; ns, not significant.

suppressing airway remodeling, improving lung function, and alleviating airway hyperresponsiveness. PLK1 inhibition significantly decreased Th17-related cytokines such as IL-17A, which play an important role in neutrophilic inflammation, suggesting these effects are likely to be associated with Th17 pathway.

The S1P signaling pathway plays a significant part in asthma pathogenesis. Elevated S1P levels in the BALF and serum of asthma patients have been observed, and metabolomic analyses have revealed a close relationship between S1P metabolic levels and asthma severity.[7] T2-high asthma with neutrophilic inflammation, often presenting with exacerbated airway neutrophil infiltration, hyperresponsiveness, remodeling, and insensitivity to steroid treatment.[2,3,22] We established a T2-high asthma with neutrophilic inflammation model using OVA sensitization and ozone exposure as previously described,[21,23] confirmed elevated S1P levels in this model, and validated the role of S1P in promoting ASMC proliferation and contraction, consistent with other studies.[16,24] Furthermore, through transcriptome sequencing, we found that PLK1, which is closely related to proliferation and contraction, was significantly upregulated in S1P-stimulated ASMCs and could serve as a key downstream molecule of S1P signaling with a central role. Inhibition of PLK1 significantly attenuated S1P-induced proliferation and contraction of ASMCs, suggesting that PLK1 may mediate the induction of ASMCs proliferation and contraction.

PLK1, which is known for its regulatory role in the cell cycle and overexpression in various cancers, has yet to be thoroughly explored in asthma, especially T2-high asthma with neutrophilic inflammation. We found that PLK1 was significantly elevated in lung tissues (including ASMCs) of the T2-high asthma with neutrophilic inflammation model, consistent with findings of Liao et al regarding heightened PLK1 protein expression in ASMCs of asthma patients.[25] According to our results, steroid (Dex) treatment could alleviate airway inflammation in the T2-high asthma with

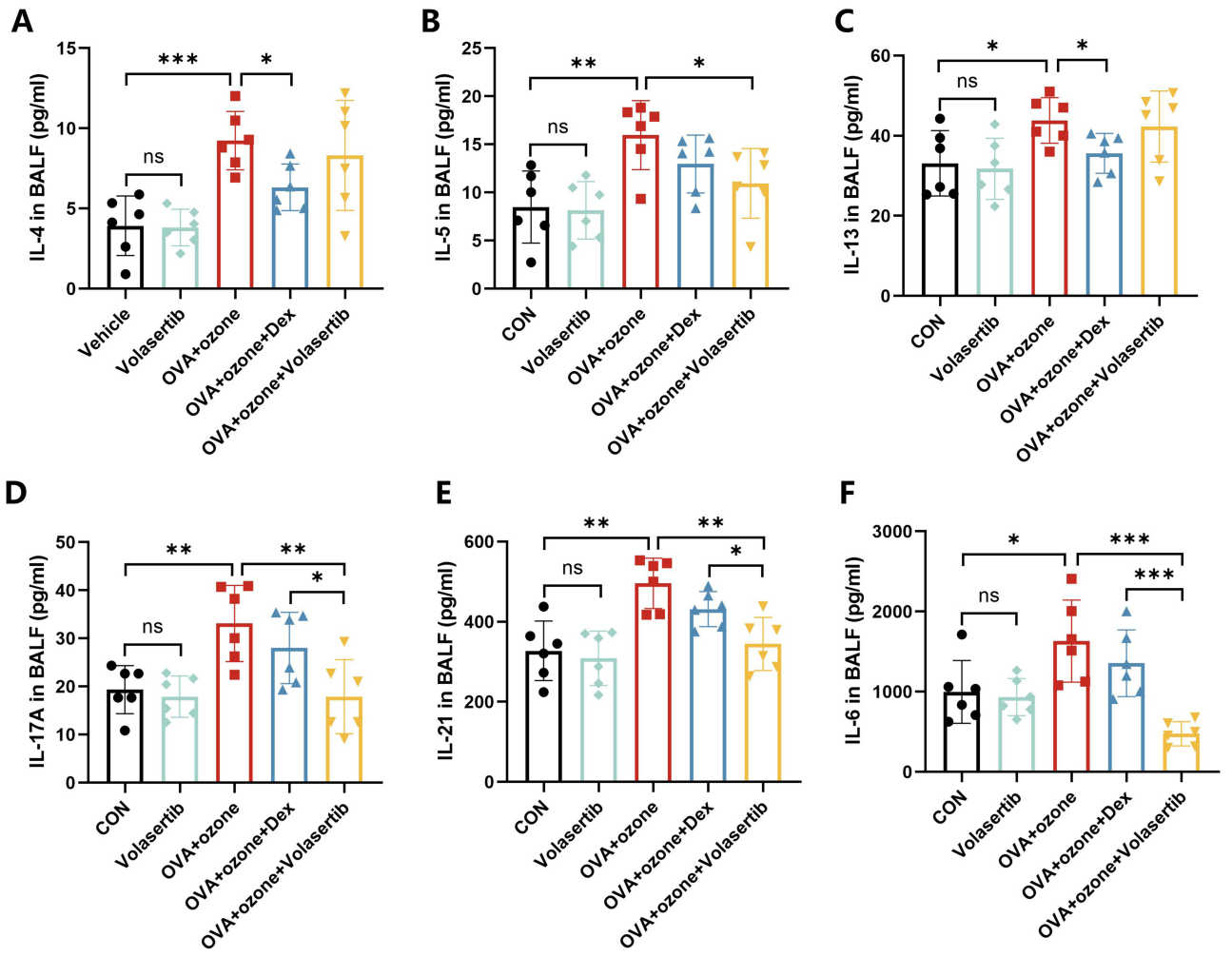

Figure 6 Effects of PLK1 inhibition on inflammatory cytokines in BALF of T2-high asthma with neutrophilic inflammation model. Cytokines in BALF were measured by ELISA. (**A**) IL-4 levels in BALF (n = 6 per group). (**B**) IL-5 levels in BALF (n = 6 per group). (**C**) IL-13 levels in BALF (n = 6 per group). (**D**) IL-6 levels in BALF (n = 6 per group). (**E**) IL-17A levels in BALF (n = 6 per group). (**F**) IL-21 levels in BALF (n = 6 per group). The error bars represent the standard deviation. *P < 0.05, **P < 0.01, ***P < 0.001.
Abbreviation: ns, not significant.

neutrophilic inflammation model but did not improve airway neutrophil infiltration, airway remodeling, airway hyperresponsiveness, or lung function. We thought the reason for dexamethasone's ineffectiveness in alleviating airway hyperresponsiveness might be that it could not effectively mitigate neutrophilic inflammation and had little impact on IL-17A levels, a key inflammatory factor that promotes neutrophilic inflammation.[26] However, after administration of volasertib, a highly selective PLK1 inhibitor, we observed significant suppression of airway neutrophil infiltration and peri-airway collagen deposition. Airway smooth muscle layer thickening, a key characteristic of asthma airway remodeling, was also notably inhibited, consistent with our in vitro study showing that inhibition of PLK1 attenuated the proliferation of ASMCs. These results were partly consistent with those of Rezey et al, who found that conditional PLK1 knockout significantly reduced airway smooth muscle layer thickening in asthmatic mice but did not inhibit airway inflammation;[27] this may have been related to different intervention methods. Our study also showed that PLK1 inhibition improved lung function (including both large and small airways) and mitigated airway resistance and hyperresponsiveness in the T2-high asthma with neutrophilic inflammation model, consistent with our cellular experiments in which inhibition of PLK1 reduced S1P-induced ASMC contraction. Various studies have reported that PLK1 can regulate the contractile function of smooth muscle cells. For instance, de Cárcer et al found that PLK1 modulated activation of the RHOA signaling pathway and actomyosin dynamics to affect contraction in vascular smooth muscle

https://doi.org/10.2147/JIR.S501645

cells;[28] Hennenberg et al reported that PLK1 promoted prostate smooth muscle cell contraction through α1-adrenergic stimulation;[20] and Li et al found that PLK1 regulated airway smooth muscle contraction via vimentin phosphorylation.[29]

Our findings, encompassing both cellular and animal models, demonstrate that PLK1 has a crucial role in the pathophysiological progression of the T2-high asthma with neutrophilic inflammation model. However, the precise mechanisms through which PLK1 affects T2-high asthma with neutrophilic inflammation, particularly its effects on cytokine profiles, remain to be elucidated. Conditional ablation of the PLK1 gene has been reported to have no significant impact on IL-13 levels in the BALF of house dust mite-induced asthmatic mice.[27] Here, we found that suppression of PLK1 did not alter levels of IL-4 and IL-13 in the BALF of our T2-high asthma with neutrophilic inflammation model, yet it led to a reduction in IL-5 levels. IL-4 and IL-13 synergistically facilitate IgE synthesis, induce production of nitric oxide and goblet cell metaplasia, enhance contractile responses, and stimulate proliferation of ASMCs.[30] They have common signaling pathways, activated by the binding of both cytokines to receptor complexes including the α-subunit of the IL-4 receptor (IL-4Rα). Our findings suggest that PLK1 might partially operate through a Th2-dependent pathway (such as IL-5) without affecting IL-4/IL-13 production. We found that dexamethasone could reduce eosinophils but has no effect on IL-5 levels. This might be because, in asthma, IL-5 is produced not only by eosinophils but also by other cells such as Th2 cells, mast cells, and monocytes. Additionally, dexamethasone may inhibit eosinophil proliferation and differentiation by reducing IL-4 and IL-13 levels, thereby decreasing eosinophils. Further, in our study, levels of IL-6, IL-17A, and IL-21 significantly decreased in the T2-high asthma with neutrophilic inflammation model after inhibition of PLK1. IL-17A and IL-21 are Th17-related cytokines that contribute to asthma pathogenesis.[31,32] Notably, IL-17A plays a crucial role in promoting neutrophilic inflammation and airway hyperresponsiveness.[26,33,34] This may explain why PLK1 inhibition could relieve airway hyperresponsiveness without reducing IL-13 levels. Signal transducer and activator of transcription 3 (STAT3) is a critical transcription factor promoting the initial differentiation of naive $CD4^+$ T cells into the Th17 cell lineage.[35] In our previous study, we found that STAT3 expression was upregulated in lung tissues of T2-high asthma with neutrophilic inflammation model and significantly correlated with expression of Th17 cytokines.[21] Studies have identified a regulatory relationship between PLK1 and STAT3, in which PLK1 inhibition downregulates STAT3 expression and phosphorylation, thereby affecting downstream signaling pathways.[36,37] However, the specific influence of PLK1 on STAT3 that affects IL-17A and IL-21 expression in T2-high asthma with neutrophilic inflammation model remains speculative. IL-6 is a key pro-inflammatory cytokine that promotes the recruitment and activation of neutrophils, exacerbating neutrophilic inflammation in the airways.[38] It is also a cytokine that plays an important part in Th17 cell differentiation.[39] Li et al demonstrated that blocking PLK1 reduced serum IL-6 levels in a lupus mouse model; this was potentially linked to diminished mTOR signal phosphorylation in spleen cell subgroups.[40] Whether a similar mechanism exists in T2-high asthma with neutrophilic inflammation is currently unclear. In summary, the results of the present study suggest that PLK1 may act predominantly through a Th17-dependent pathway.

Our study had several limitations. First, owing to constraints, we were unable to measure PLK1 levels in the serum, BALF, or lung tissues of asthma patients or compare these with healthy individuals. Second, we conducted an observational study on the association between PLK1 inhibition and the T2-high asthma with neutrophilic inflammation endotype, as well as preliminary exploration at the cytokine level. The potential associative mechanism between PLK1 and T2-high asthma with neutrophilic inflammation requires more in-depth research.

Conclusion

PLK1 mediates S1P-induced proliferation and contraction of ASMCs and is elevated in a T2-high asthma with neutrophilic inflammation model. Inhibition of PLK1 could improve airway inflammation, remodeling, and hyperresponsiveness in the T2-high asthma with neutrophilic inflammation model, potentially through Th17-related cytokines such as IL-17A. PLK1 holds promise as a potential therapeutic target for T2-high asthma with neutrophilic inflammation, and its specific molecular mechanisms require further investigation.

Data Sharing Statement

The datasets generated during the current study are available from the corresponding author upon reasonable request.

Ethics Approval and Consent to Participate

The animal study (IACUC: 2023AW334) was approved by the Ethics Committee of Shanghai General Hospital, Shanghai Jiao Tong University School of Medicine.

Author Contributions

All authors made a significant contribution to the work reported, whether that is in the conception, study design, execution, acquisition of data, analysis and interpretation, or in all these areas; took part in drafting, revising or critically reviewing the article; gave final approval of the version to be published; have agreed on the journal to which the article has been submitted; and agree to be accountable for all aspects of the work.

Funding

The work was supported by Shanghai Sailing Program [grant number 22YF1434900], the Fundamental Research Funds for the Central Universities [grant number YG2023QNA28], Zhongnanshan Medical Foundation of Guangdong Province [grant number ZNSXS-20240002], and Clinical Research Innovation Plan of Shanghai General Hospital [grant number CCTR-2023C04].

Disclosure

The authors report no conflicts of interest in this work.

References

1. Reddel HK, Bacharier LB, Bateman ED, et al. Global initiative for asthma strategy 2021: executive summary and rationale for key changes. *Eur Respir J*. 2022;59(1):2102730. doi:10.1183/13993003.02730-2021
2. Wu W, Bleecker E, Moore W, et al. Unsupervised phenotyping of severe asthma research program participants using expanded lung data. *J Allergy Clin Immunol*. 2014;133(5):1280–1288. doi:10.1016/j.jaci.2013.11.042
3. Moore WC, Hastie AT, Li X, et al. Sputum neutrophil counts are associated with more severe asthma phenotypes using cluster analysis. *J Allergy clin Immunol*. 2014;133(6):1557–63e5. doi:10.1016/j.jaci.2013.10.011
4. Morad SA, Cabot MC. Ceramide-orchestrated signalling in cancer cells. *Nat Rev Cancer*. 2013;13(1):51–65. doi:10.1038/nrc3398
5. Wang HC, Wong TH, Wang LT, et al. Aryl hydrocarbon receptor signaling promotes ORMDL3-dependent generation of sphingosine-1-phosphate by inhibiting sphingosine-1-phosphate lyase. *Cell mol Immunol*. 2019;16(10):783–790. doi:10.1038/s41423-018-0022-2
6. Ammit AJ, Hastie AT, Edsall LC, et al. Sphingosine 1-phosphate modulates human airway smooth muscle cell functions that promote inflammation and airway remodeling in asthma. *FASEB J*. 2001;15(7):1212–1214. doi:10.1096/fj.00-0742fje
7. Reinke SN, Gallart-Ayala H, Gomez C, et al. Metabolomics analysis identifies different metabotypes of asthma severity. *Eur Respir J*. 2017;49(3):1601740. doi:10.1183/13993003.01740-2016
8. Rahman MM, Alkhouri H, Tang F, Che W, Ge Q, Ammit AJ. Sphingosine 1-phosphate induces neutrophil chemoattractant IL-8: repression by steroids. *PLoS One*. 2014;9(3):e92466. doi:10.1371/journal.pone.0092466
9. Roviezzo F, Sorrentino R, Bertolino A, et al. S1P-induced airway smooth muscle hyperresponsiveness and lung inflammation in vivo: molecular and cellular mechanisms. *Br J Pharmacol*. 2015;172(7):1882–1893. doi:10.1111/bph.13033
10. Terashita T, Kobayashi K, Nagano T, et al. Administration of JTE013 abrogates experimental asthma by regulating proinflammatory cytokine production from bronchial epithelial cells. *Respir Res*. 2016;17(1):146. doi:10.1186/s12931-016-0465-x
11. Roviezzo F, Sorrentino R, Iacono VM, et al. Disodium cromoglycate inhibits asthma-like features induced by sphingosine-1-phosphate. *Pharmacol Res*. 2016;113(Pt A):626–635. doi:10.1016/j.phrs.2016.09.014
12. Roviezzo F, Di Lorenzo A, Bucci M, et al. Sphingosine-1-phosphate/sphingosine kinase pathway is involved in mouse airway hyperresponsiveness. *Am J Respir Cell mol Biol*. 2007;36(6):757–762. doi:10.1165/rcmb.2006-0383OC
13. Fuerst E, Foster HR, Ward JP, Corrigan CJ, Cousins DJ, Woszczek G. Sphingosine-1-phosphate induces pro-remodelling response in airway smooth muscle cells. *Allergy*. 2014;69(11):1531–1539. doi:10.1111/all.12489
14. Bao W, Zhang Y, Zhang M, et al. Effects of ozone repeated short exposures on the airway/lung inflammation, airway hyperresponsiveness and mucus production in a mouse model of ovalbumin-induced asthma. *Biomed Pharmacother*. 2018;101:293–303. doi:10.1016/j.biopha.2018.02.079
15. Xue Y, Bao W, Zhou Y, et al. Small-airway dysfunction is involved in the pathogenesis of asthma: evidence from two mouse models. *J Asthma Allergy*. 2021;14:883–896. doi:10.2147/JAA.S312361
16. Pan Y, Liu L, Zhang Q, et al. Activation of AMPK suppresses S1P-induced airway smooth muscle cells proliferation and its potential mechanisms. *Mol Immunol*. 2020;128:106–115. doi:10.1016/j.molimm.2020.09.020
17. Pan Y, Liu L, Li S, et al. Activation of AMPK inhibits TGF-beta1-induced airway smooth muscle cells proliferation and its potential mechanisms. *Sci Rep*. 2018;8(1):3624. doi:10.1016/j.jaci.2023.05.028
18. Toumpanakis D, Usmani O. Small airways in asthma: pathophysiology, identification and management. *Chin M J Pulm Crit Care Med*. 2023;1:171–180. doi:10.1016/j.pccm.2023.07.002
19. Elsayed I, Wang X. PLK1 inhibition in cancer therapy: potentials and challenges. *Future Med Chem*. 2019;11(12):1383–1386. doi:10.4155/fmc-2019-0084

20. Hennenberg M, Kuppermann P, Yu Q, et al. Inhibition of prostate smooth muscle contraction by inhibitors of polo-like kinases. *Front Physiol*. 2018;9:734. doi:10.3389/fphys.2018.00734
21. Xue Y, Zhou Y, Bao W, et al. STAT3 and IL-6 contribute to corticosteroid resistance in an OVA and ozone-induced asthma model with neutrophil infiltration. *Front Mol Biosci*. 2021;8:717962. doi:10.3389/fmolb.2021.717962
22. Moore WC, Meyers DA, Wenzel SE, et al. Identification of asthma phenotypes using cluster analysis in the severe asthma research program. *Am J Respir Crit Care Med*. 2010;181(4):315–323. doi:10.1164/rccm.200906-0896OC
23. Zhou Y, Qiu Y, Bao W, et al. Evaluating the effects of vitamin D Level on airway obstruction in two asthma endotypes in humans and in two mouse models with different intake of vitamin D during early-life. *Front Immunol*. 2023;14:1107031. doi:10.3389/fimmu.2023.1107031
24. Maguire TJA, Yung S, Ortiz-Zapater E, et al. Sphingosine-1-phosphate induces airway smooth muscle hyperresponsiveness and proliferation. *J Allergy Clin Immunol*. 2023;152(5):1131–40e6.
25. Liao G, Wang R, Rezey AC, Gerlach BD, Tang DD. MicroRNA miR-509 regulates ERK1/2, the Vimentin network, and focal adhesions by targeting Plk1. *Sci Rep*. 2018;8(1):12635. doi:10.1038/s41598-018-30895-8
26. Chesne J, Braza F, Mahay G, Brouard S, Aronica M, Magnan A. IL-17 in severe asthma. Where do we stand? *Am J Respir Crit Care Med*. 2014;190(10):1094–1101. doi:10.1164/rccm.201405-0859PP
27. Rezey AC, Gerlach BD, Wang R, Liao G, Tang DD. Plk1 mediates paxillin phosphorylation (Ser-272), centrosome maturation, and airway smooth muscle layer thickening in allergic asthma. *Sci Rep*. 2019;9(1):7555. doi:10.1038/s41598-019-43927-8
28. de Carcer G, Wachowicz P, Martinez-Martinez S, et al. Plk1 regulates contraction of postmitotic smooth muscle cells and is required for vascular homeostasis. *Nat Med*. 2017;23(8):964–974. doi:10.1038/nm.4364
29. Li J, Wang R, Gannon OJ, et al. Polo-like kinase 1 regulates vimentin phosphorylation at Ser-56 and contraction in smooth muscle. *J Biol Chem*. 2016;291(45):23693–23703. doi:10.1074/jbc.M116.749341
30. Lambrecht BN, Hammad H, Fahy JV. The cytokines of asthma. *Immunity*. 2019;50(4):975–991. doi:10.1016/j.immuni.2019.03.018
31. Gupta RK, Gupta K, Dwivedi PD. Pathophysiology of IL-33 and IL-17 in allergic disorders. *Cytokine Growth Factor Rev*. 2017;38:22–36. doi:10.1016/j.cytogfr.2017.09.005
32. Saadh MJ, Alfattah MA, Ismail AH, et al. The role of Interleukin-21 (IL-21) in allergic disorders: biological insights and regulatory mechanisms. *Int Immunopharmacol*. 2024;134:111825. doi:10.1016/j.intimp.2024.111825
33. Chiba Y, Tanoue G, Suto R, et al. Interleukin-17A directly acts on bronchial smooth muscle cells and augments the contractility. *Pharmacol Rep*. 2017;69(3):377–385. doi:10.1016/j.pharep.2016.12.007
34. Mizutani N, Nabe T, Yoshino S. IL-17A promotes the exacerbation of IL-33-induced airway hyperresponsiveness by enhancing neutrophilic inflammation via CXCR2 signaling in mice. *J Immunol*. 2014;192(4):1372–1384. doi:10.4049/jimmunol.1301538
35. Luckheeram RV, Zhou R, Verma AD, Xia B. CD4(+)T cells: differentiation and functions. *Clin Dev Immunol*. 2012;2012:925135. doi:10.1155/2012/925135
36. Zhang Y, Du XL, Wang CJ, et al. Reciprocal activation between PLK1 and Stat3 contributes to survival and proliferation of esophageal cancer cells. *Gastroenterology*. 2012;142(3):521–30e3. doi:10.1053/j.gastro.2011.11.023
37. Yu C, Luo D, Yu J, et al. Genome-wide CRISPR-cas9 knockout screening identifies GRB7 as a driver for MEK inhibitor resistance in KRAS mutant colon cancer. *Oncogene*. 2022;41(2):191–203. doi:10.1038/s41388-021-02077-w
38. Hudey SN, Ledford DK, Cardet JC. Mechanisms of non-type 2 asthma. *Curr Opin Immunol*. 2020;66:123–128. doi:10.1016/j.coi.2020.10.002
39. Chandran S, Tang Q. Impact of interleukin-6 on T cells in kidney transplant recipients. *Am J Transplant*. 2022;22(Suppl 4):18–27. doi:10.1111/ajt.17209
40. Li Y, Wang H, Zhang Z, et al. Identification of polo-like kinase 1 as a therapeutic target in murine lupus. *Clin Transl Immunology*. 2022;11(1):e1362. doi:10.1002/cti2.1362